Al2O3 and TiO2 Atomic Layer Deposition on Copper for Water Corrosion Resistance

9 AUTHORS, INCLUDING:

Aziz Abdulagatov
National Institute of Standards and Technol…

38 PUBLICATIONS   **432** CITATIONS

Zachary M Gibbs
California Institute of Technology

36 PUBLICATIONS   **369** CITATIONS

Andrew Cavanagh
University of Colorado Boulder

49 PUBLICATIONS   **1,692** CITATIONS

Ronggui Yang
University of Colorado Boulder

167 PUBLICATIONS   **3,570** CITATIONS

Al$_2$O$_3$ and TiO$_2$ Atomic Layer Deposition on Copper for Water Corrosion Resistance

A. I. Abdulagatov,[†] Y. Yan,[‡] J. R. Cooper,[‡] Y. Zhang,[‡] Z. M. Gibbs,[§] A. S. Cavanagh,[⊥] R. G. Yang,[‡] Y. C. Lee,[‡,#] and S. M. George*,[†,§]

[†]Department of Chemistry and Biochemistry, [‡]Department of Mechanical Engineering, [§]Department of Chemical and Biological Engineering, [⊥]Department of Physics, and [#]DARPA Center for Integrated Micro/Nano-Electromechanical Transducers (iMINT), University of Colorado, Boulder, Colorado 80309-0215, United States

ABSTRACT: Al$_2$O$_3$ and TiO$_2$ atomic layer deposition (ALD) were employed to develop an ultrathin barrier film on copper to prevent water corrosion. The strategy was to utilize Al$_2$O$_3$ ALD as a pinhole-free barrier and to protect the Al$_2$O$_3$ ALD using TiO$_2$ ALD. An initial set of experiments was performed at 177 °C to establish that Al$_2$O$_3$ ALD could nucleate on copper and produce a high-quality Al$_2$O$_3$ film. In situ quartz crystal microbalance (QCM) measurements verified that Al$_2$O$_3$ ALD nucleated and grew efficiently on copper-plated quartz crystals at 177 °C using trimethylaluminum (TMA) and water as the reactants. An electroplating technique also established that the Al$_2$O$_3$ ALD films had a low defect density. A second set of experiments was performed for ALD at 120 °C to study the ability of ALD films to prevent copper corrosion. These experiments revealed that an Al$_2$O$_3$ ALD film alone was insufficient to prevent copper corrosion because of the dissolution of the Al$_2$O$_3$ film in water. Subsequently, TiO$_2$ ALD was explored on copper at 120 °C using TiCl$_4$ and water as the reactants. The resulting TiO$_2$ films also did not prevent the water corrosion of copper. Fortunately, Al$_2$O$_3$ films with a TiO$_2$ capping layer were much more resilient to dissolution in water and prevented the water corrosion of copper. Optical microscopy images revealed that TiO$_2$ capping layers as thin as 200 Å on Al$_2$O$_3$ adhesion layers could prevent copper corrosion in water at 90 °C for ∼80 days. In contrast, the copper corroded almost immediately in water at 90 °C for Al$_2$O$_3$ and ZnO films by themselves on copper. Ellipsometer measurements revealed that Al$_2$O$_3$ films with a thickness of ∼200 Å and ZnO films with a thickness of ∼250 Å dissolved in water at 90 °C in ∼10 days. In contrast, the ellipsometer measurements confirmed that the TiO$_2$ capping layers with thicknesses of ∼200 Å on the Al$_2$O$_3$ adhesion layers protected the copper for ∼80 days in water at 90 °C. The TiO$_2$ ALD coatings were also hydrophilic and facilitated H$_2$O wetting to copper wire mesh substrates.
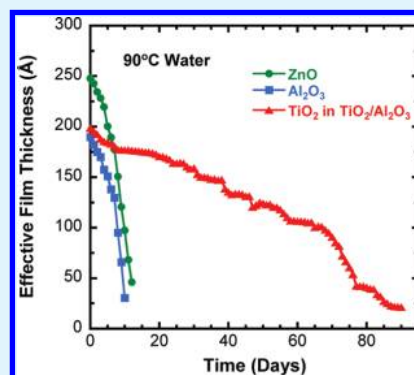
KEYWORDS: atomic layer deposition, copper, corrosion, Al$_2$O$_3$, TiO$_2$, water

1. INTRODUCTION

Copper is an important structural material with a high thermal conductivity. Copper is used extensively in plumbing water and for water heat exchangers. Although copper has a reasonable water corrosion resistance, finite corrosion rates of ∼1 mg/dm^2/day occur in pure water with 1 mL/L oxygen concentration.[1] The corrosion occurs by means of an electrochemical mechanism in which areas remote from one another on an atomic scale serve as anodes and cathodes.[2,3] Copper corrosion is dependent on solutes in water,[4–6] the pH of water,[5,7] and the water temperature.[4,8]

Many gas phase and wet chemical techniques have been employed to protect copper from corrosion. Previous attempts have utilized coatings deposited by chemical vapor deposition (CVD).[9,10] In addition, copper surfaces have been chemically protected using wet chemical treatments using self-assembled monolayers,[11–13] organic azoles,[14–16] and polymers.[17–19] Other approaches for copper corrosion protection have utilized plasma[20] and electrochemical[21] deposition techniques. All of these methods have their limitations and may not be robust enough to prevent copper corrosion in water at elevated temperatures.

In this paper, Al$_2$O$_3$ and TiO$_2$ atomic layer deposition (ALD) coatings on copper were explored as ultrathin protective coatings to prevent corrosion by water. ALD is a gas phase coating technique based on sequential, self-limiting surface chemical reactions.[22] ALD can provide atomic level control of film thickness and deposit extremely conformal coatings on high-aspect-ratio structures.[22,23] Al$_2$O$_3$ is a well-defined ALD system and is performed using trimethylaluminum (TMA) and H$_2$O.[24–26] Al$_2$O$_3$ ALD has been used previously as a corrosion resistant coating.[27,28] TiO$_2$ ALD is also a well-established ALD system and is accomplished using TiCl$_4$ and H$_2$O.[29] TiO$_2$ ALD has been reported to protect stainless steel[27,30] and CrN[31] from electrochemical corrosion.

Al$_2$O$_3$ ALD is known to form nearly pinhole-free films.[32] Al$_2$O$_3$ ALD has also been shown to be an excellent gas diffusion barrier on polymers.[33–35] Recent measurements of the water vapor transmission rate (WVTR) through Al$_2$O$_3$ films on

polymer have demonstrated that Al_2O_3 ALD films with thicknesses of >10 nm have equivalent barrier properties to glass.[33] Al_2O_3 ALD films can also protect polymers from atomic oxygen and vacuum ultraviolet (VUV) attack.[36,37] However, Al_2O_3 ALD films are susceptible to corrosion by water.[38] Consequently, the Al_2O_3 ALD barrier must be protected to prevent water corrosion. TiO_2 is known to display excellent water resistance.[39,40] TiO_2 ALD can be used to protect the Al_2O_3 ALD layer from water corrosion.

The nucleation and growth of Al_2O_3 ALD on copper at 177 °C was studied using in situ quartz crystal microbalance (QCM) measurements to confirm that Al_2O_3 ALD grows efficiently on copper surfaces. The pinhole density in the Al_2O_3 ALD coatings on copper was also measured using electroplating techniques. Optical microscopy was employed to monitor copper corrosion in water at 25 and 90 °C using Al_2O_3 ALD, TiO_2 ALD, and TiO_2/Al_2O_3 ALD coatings grown at 120 °C. Ellipsometry studies also observed the film thickness of Al_2O_3, TiO_2, ZnO, and TiO_2/Al_2O_3 coatings versus time in water at 90 °C. Contact angle measurements characterized H_2O wetting on TiO_2-coated copper wire mesh substrates.

2. EXPERIMENTAL SECTION

Al_2O_3, TiO_2, and ZnO ALD were performed in a viscous-flow, hot-wall type ALD reactor described in detail elsewhere.[41] The Al_2O_3 ALD was deposited using 97% pure TMA (Sigma-Aldrich, U.S.A.) and chromatography-grade water at 120 and 177 °C. Nucleation on copper substrates was explored at the optimum growth temperature of 177 °C for Al_2O_3 ALD.[25] Al_2O_3 ALD films were deposited at 120 °C for the studies of copper corrosion. This lower temperature was employed because this study was motivated by the problem of copper corrosion in microelectromechanical systems (MEMS) devices that contain thermally sensitive polymers.[42]

The TiO_2 ALD was deposited using 98% pure $TiCl_4$ (Strem Chemicals Inc., U.S.A.) and water at 120 °C. Titanium tetrachloride is a stable precursor with good vapor pressure at room temperature and was considered the best metal precursor for TiO_2 deposition. TiO_2 ALD using titanium(IV) isopropoxide and H_2O was not employed because this system requires temperatures from 250 to 325 °C[43] that are not compatible with most polymers. Titanium(IV) dimethylamaide (TDMAT) and H_2O was not used for TiO_2 ALD because TDMAT has thermal decomposition problems and is known to yield very poor TiN ALD films at low temperatures.[44]

The ZnO ALD was deposited using diethylzinc (Sigma-Aldrich, U.S.A.) and H_2O at 120 °C. During Al_2O_3, TiO_2 and ZnO ALD, the metal precursors and H_2O were maintained at room temperature. Ultra high purity (99.999%) grade nitrogen (Airgas, CO, U.S.A.) was used as the purge and carrier gas in the ALD reactor. With pumping using a mechanical pump, the flowing N_2 gas defined a base pressure of 0.9 Torr. All the films in this paper were grown using ALD techniques unless stated otherwise.

QCM measurements were performed using AT- cut, 6 MHz resonant frequency, unpolished, copper-plated quartz crystal sensors (Inficon Inc.,U.S.A.). The QCM sensor was coated with a 7 μm thick copper film. Copper was deposited using electron beam evaporation. A layer of titanium with a thickness of 200 Å served as the adhesion layer between the quartz crystal and the copper film. The QCM crystal was mounted in a bakeable sensor housing and sealed using high temperature conductive epoxy and purged with nitrogen to prevent deposition on the backside of the crystal.[41] The copper-plated crystal turned a bright red color, indicating the presence of thick layer of copper oxide, after epoxy curing in the QCM housing in air at 200 °C for two hours. Typically, copper

heated to 200 °C in air has as a oxide layer consisting of a mixture of Cu(I) and Cu(II).[45]

Precut, copper-plated, silicon wafers with dimensions of 2.5 cm × 2.5 cm were used as the copper substrates for the copper corrosion studies. These wafers were covered with a 15 μm polished copper film deposited using electron beam evaporation. The copper was evaporated onto a 250 Å thick tantalum adhesion layer (Montco Silicon Technologies Inc., U.S.A.). X-ray photoelectron spectroscopy (XPS) analysis of these copper substrates indicated the presence of a native oxide layer in the Cu(I) oxidation state. The thickness of the Cu_2O oxide layer was determined to be ~30 Å using spectroscopic ellipsometry. All of the substrates referred to in this work as copper were assumed to have a native copper oxide on the surface.

A spectroscopic ellipsometer (J. A. Woollam Co., U.S.A.) was used to determine the thickness and refractive index of the deposited TiO_2 and Al_2O_3 films. The thickness was measured using three different wavelengths (418.5, 594.6, and 763.2 nm) at an incident angle of 75°. Refractive indexes of deposited TiO_2 and Al_2O_3 were obtained using the Tauc-Lorentz and Cauchy models, respectively. A Gaertner Ellipsometer L117 (Skokie, Illinois, U.S.A.) was used to monitor changes in film thickness after immersion in water. The thickness was obtained at three different locations for each measurement.

Auger electron spectroscopy (AES) and X-ray photoelectron spectroscopy (XPS) were used to examine the composition of the Al_2O_3 ALD film on copper surfaces. AES measurements were conducted at the University of Minnesota College of Science and Engineering Characterization Facility on a Physical Electronics scanning Auger spectrometer (PHI model 545). Depth profile data was obtained with 3 keV Ar^+ sputtering. XPS scans were performed at the University of Colorado using a Physical Electronics (PHI model 5600) spectrometer with a monochromatic Al Kα X-ray source with energy of 1486.6 eV. XPS survey scans were performed with an electron pass energy of 187 eV and a resolution of 0.8 eV.

Surface morphologies of the ALD films deposited on copper substrates were determined using atomic force microscopy (AFM). Measurements were performed using an Autoprobe CP instrument from Thermomicroscopes atop an air table (Integrated Dynamics Engineering, U.S.A.). AFM images were acquired in noncontact mode. All scans were 5 μm × 5 μm and performed at a scan rate of 0.8 Hz using "A" tip rectangular cantilevers (MikroMasch Company, U.S.A.).

Copper electroplating was utilized to visualize defects in the Al_2O_3 ALD films deposited on copper.[46] The electroplating solvent was composed of 1.0 M H_2SO_4 and 0.4 M $CuSO_4$.[46] Because Al_2O_3 is a dielectric, copper only grew at defect sites in the Al_2O_3 film where the electrolytic solution established contact with the conductive substrate during electroplating. After the electroplating, the defects were revealed as copper bumps. These defects were analyzed and counted using optical (Nikon ECLIPSE LV150, Japan) and scanning electron microscopy (SEM) (Jeol Limited JSM-6480LV, Japan) techniques.

Corrosion protection properties of the ALD films were investigated by immersing coated substrates into chromatography grade water at room temperature and 90 °C. Coated copper substrates were fully immersed in water that was heated to a precision of ±2.5 °C using a hot plate (Thermo Fisher Scientific Inc., U.S.A.). After sample removal and prior to any analysis, the samples were dried with nitrogen gas. Thickness data and optical images of the copper substrates were measured every 1−4 days. An optical microscope (Nikon ECLIPSE LV150, Japan) was used to record the optical images.

The optical images were analyzed using ImageJ.[47] All of the images of the bare and coated copper substrates were obtained under the same conditions and recorded with 10× magnification and 1280 × 1024 capture resolution. The images were recorded at the same region of the sample versus time to track the changes. The images were made binary by the ImageJ processing software. The average greyscale intensity of the copper
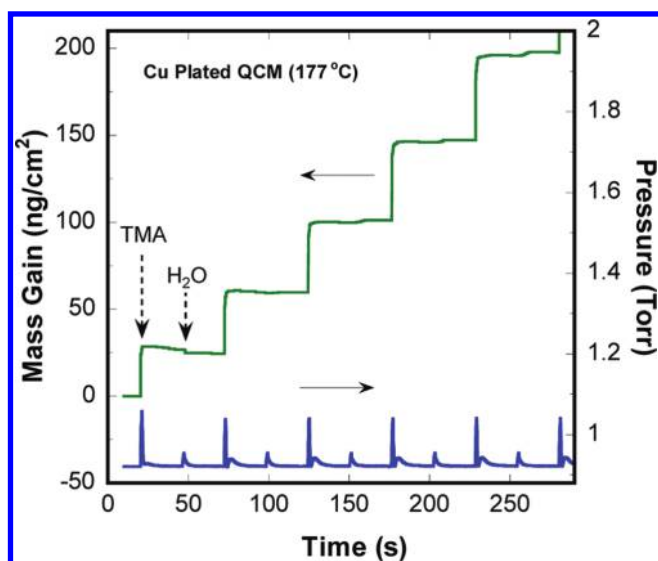
4594

dx.doi.org/10.1021/am2009579 |*ACS Appl. Mater. Interfaces* 2011, 3, 4593–4601

Figure 1. Mass gain versus time recorded during first five Al_2O_3 ALD cycles on copper-plated QCM sensor at 177 °C.

substrates before water immersion was used as the reference to define the threshold level. The copper corrosion area was defined as the relative fraction of pixels in the image that had a greyscale intensity above the threshold.

The wettability of TiO_2-coated copper meshes with 50 μm wire diameters was examined using water contact angle measurements. The contact angle was measured using 1 μL water droplets. The images were processed using First Ten Angstroms imaging software (First Ten Angstroms, Inc., U.S.A.).

3. RESULTS AND DISCUSSION

A. Nucleation and Growth of Al_2O_3 ALD on Copper. Al_2O_3 ALD on copper was investigated at 177 °C on a QCM with a copper-plated quartz crystal. The dose times for TMA and H_2O were 1 s with 30 s purge times after each pulse. TMA and H_2O exposures were 12×10^4 L (1 L $= 1 \times 10^{-6}$ Torr s) and 4×10^4 L, respectively. Figure 1 shows the QCM response during the first 5 ALD cycles. Al_2O_3 nucleates readily on the copper substrate. In the first cycle, the TMA dose resulted in a mass gain of 27 ng/cm^2 and the water dose resulted in a mass loss of 2 ng/cm^2. The total mass gain per cycle (MGPC) was 25 ng/cm^2/cycle. Figure 1 shows that the total mass gain increases progressively through the first 5 cycles.

Figure 2a displays the mass gains for TMA (Δm_A), H_2O (Δm_B) and Al_2O_3 ($\Delta m_A + \Delta m_B$) for 205 ALD cycles. Nucleation occurs over the first 15—20 ALD cycles. The total mass gain increases and reaches a maximum value of ~68 ng/cm^2/cycle. Figure 2b shows the $\Delta m_A/\Delta m_B$ ratio for individual mass gains of TMA and water. The $\Delta m_A/\Delta m_B$ ratio starts at a high value and quickly decreases and levels off at a steady state value of ~13 after 20 cycles. The negative value of the ratio on the first cycle is due to the initial mass loss during first water dose. The steady state ratio value of ~13 is slightly higher than the ratio of ~10 observed earlier during Al_2O_3 ALD on a polished, gold-plated, QCM crystal under the same reaction conditions.[41]

The QCM profiles shown in Figure 1 are consistent with the chemistry for Al_2O_3 ALD growth using TMA and water.[41,48] However, the Al_2O_3 growth rate of ~65 ng/cm^2/cycle observed
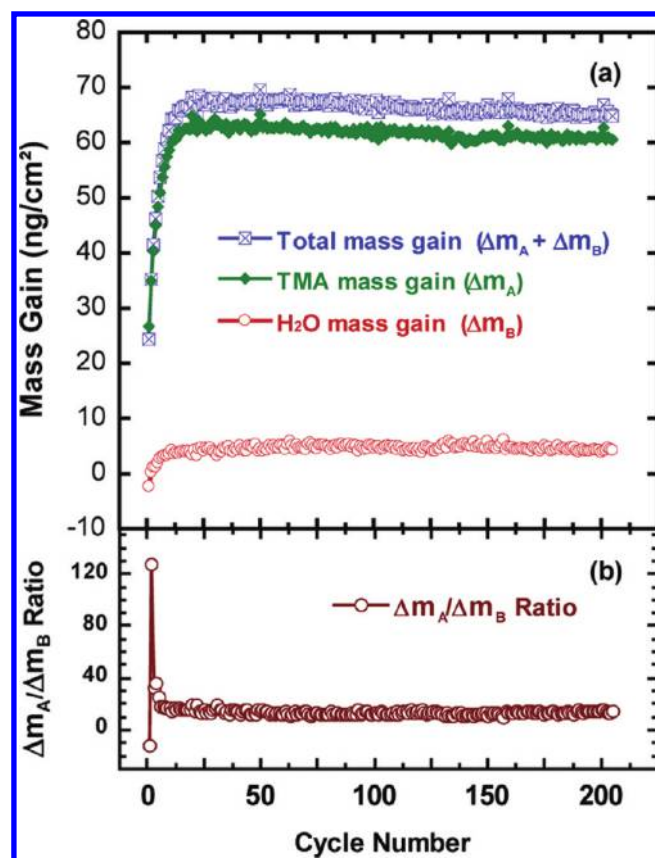

Figure 2. (a) Mass gain versus cycle number for Al_2O_3 ALD on copper-plated QCM sensor at 177 °C showing TMA mass gain, H_2O mass gain and total mass gain. (b) Ratio of the TMA mass gain and the H_2O mass gain versus cycle number for the mass gains shown in a.

after the nucleation period is about 2 times higher than the growth rate observed on polished QCM sensors. This higher mass gain per cycle is attributed to the difference in surface area between the polished and unpolished QCM sensors.[41] As the roughness of the QCM crystal surface decreases with the number of ALD cycles, the Al_2O_3 ALD MGPC should approach a MGPC of ~38 ng/cm^2/cycle that has been reported for polished QCM sensors at 177 °C.[41,48] Slightly smaller MGPCs ranging from 31 to 37 ng/cm^2/cycle are observed at 125 °C depending on TMA and H_2O exposures.[49]

The slow Al_2O_3 growth during the first several ALD cycles indicates that the surface of the copper oxide on the copper substrate may have few hydroxyl groups. Another possibility is that the copper oxide surface may be covered with carbonaceous species. There was no attempt to clean the copper oxide surface prior to the Al_2O_3 ALD. Nucleation periods of 10—20 cycles are similar to the nucleation periods observed for Al_2O_3 ALD on a variety of polymer substrates.[50]

B. Characterization of Al_2O_3 ALD Films on Copper. The thickness of the Al_2O_3 films deposited on copper was measured using ellipsometry. Measurements of the film thickness versus number of cycles yielded an Al_2O_3 ALD growth rate of 1.2 Å/cycle at 177 °C. This value is in good agreement with the growth rate observed for Al_2O_3 ALD on silicon substrates.[25] The color of the copper substrate coated with 620 Å of Al_2O_3 was deep red. The refractive index of 1.6 at 633 nm for the Al_2O_3 film deposited on copper matched previously reported values for Al_2O_3 ALD films.[48]
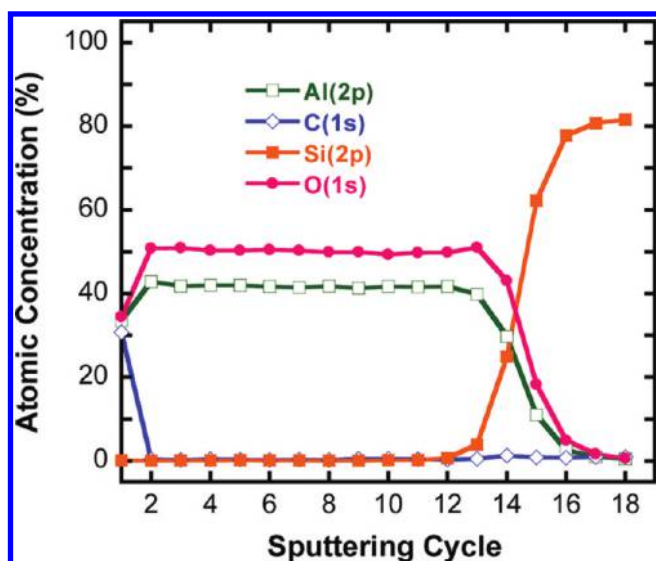
Figure 3. Atomic concentration versus sputtering cycle for Al_2O_3 ALD film with a thickness of 620 Å deposited on copper substrate at 177 °C.

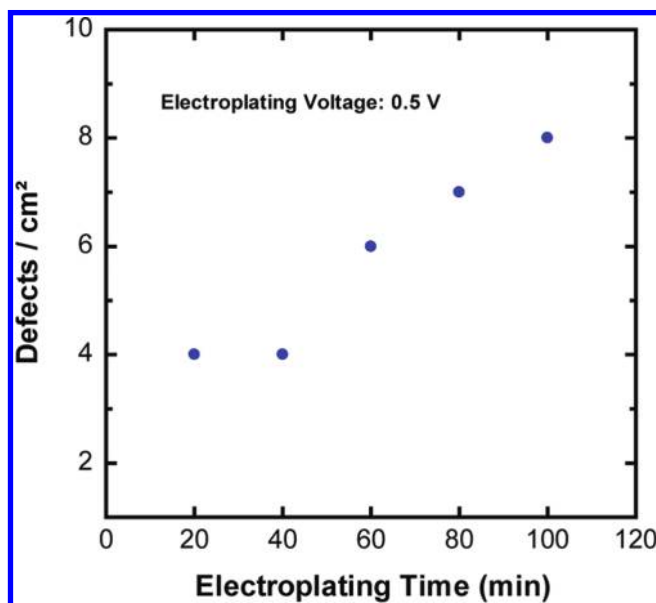**Figure 4.** Defect density versus electroplating time for Al_2O_3 ALD film with a thickness of 250 Å deposited on copper substrate at 177 °C.

Figure 5. AFM images of: (a) 300 cycles of TiO_2 ALD grown on copper substrate at 120 °C; and (b) TiO_2 capping layer with a thickness of 180 Å on Al_2O_3 adhesion layer with a thickness of 40 Å grown on copper substrate at 120 °C.

Auger electron spectroscopy (AES) was used to examine the chemical composition of the Al_2O_3 ALD film. Figure 3 displays the AES depth profile of a 620 Å thick Al_2O_3 film deposited on a copper substrate at 177 °C. There is a uniform distribution of aluminum and oxygen atoms throughout the entire film with no traces of copper in the bulk of the film. The deviation from stoichiometric Al_2O_3 with slightly lower oxygen than expected can be attributed to the preferential sputtering of light atoms during the AES depth profile. Impurities in the film were below the detection limit of the instrument.

Pinholes in the Al_2O_3 ALD film on copper were evaluated using an electroplating technique.[46] Al_2O_3 samples were prepared by deposition of Al_2O_3 films with a thickness of 250 Å on 4 in. copper wafers at 177 °C using the same reaction conditions as employed for the QCM studies. UHP grade nitrogen was used to
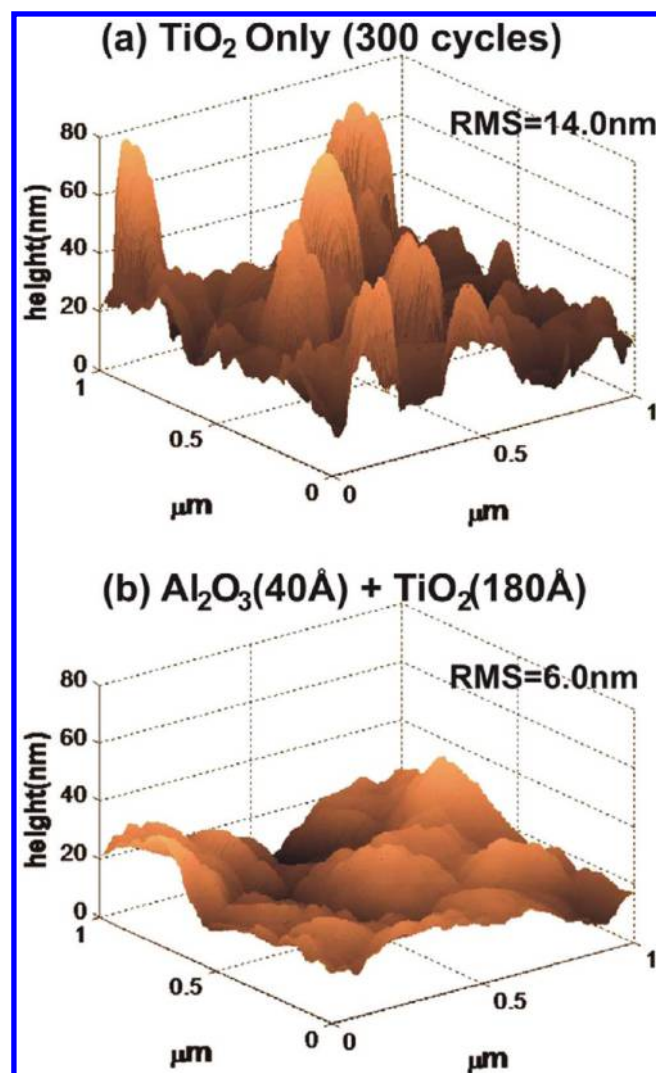
remove residual particles from the surface of the copper substrate. The copper substrate was then loaded into an ALD reactor that was larger than the ALD reactor that was used for the other ALD coatings. This larger ALD reactor was housed in a class 100 clean room environment. The substrate was placed in the ALD reactor for 30 min to allow for temperature equilibration prior to the start of the Al_2O_3 ALD.

The Al_2O_3-coated copper substrates were then subjected to electroplating prior to examination by SEM. Very few defects as revealed by copper bumps were observed after the electroplating process. Only ~4 defects per cm^2 were observed after 20 min of electroplating time. Figure 4 shows that the number of defects increases with the increase in electroplating time. After 100 min of electroplating, the Al_2O_3 ALD film on copper had only 8 defects per cm^2. This defect density compares with the lowest density of 38 defects per cm^2 obtained earlier under the same electroplating conditions for Al_2O_3 ALD films with a thickness of 250 Å deposited on nickel substrates.[46] The nickel substrates were formed by the resistive evaporation of nickel on silicon wafers.
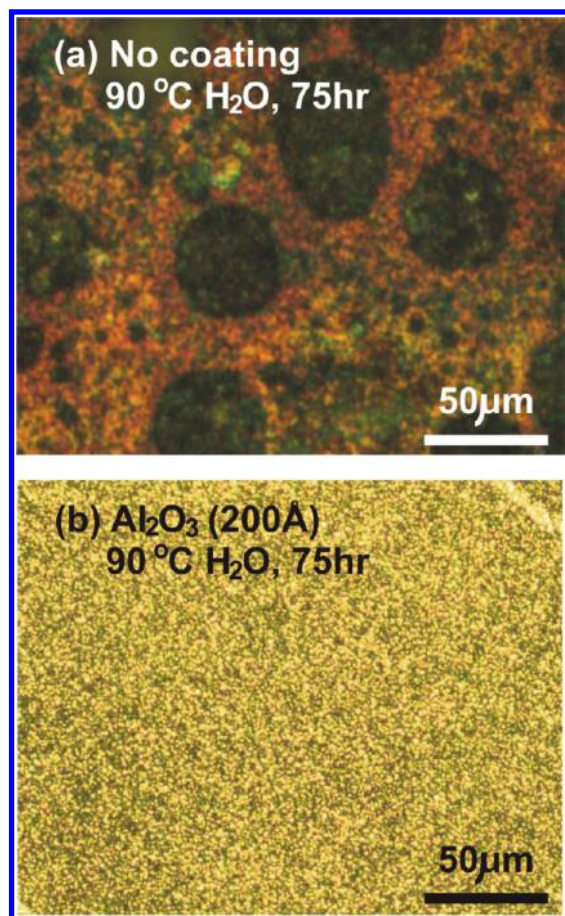
Figure 6. Optical microscope images of copper substrates after 75 h in water at 90 °C with: (a) no coating; and (b) Al_2O_3 ALD coating with thickness of 200 Å grown at 120 °C.
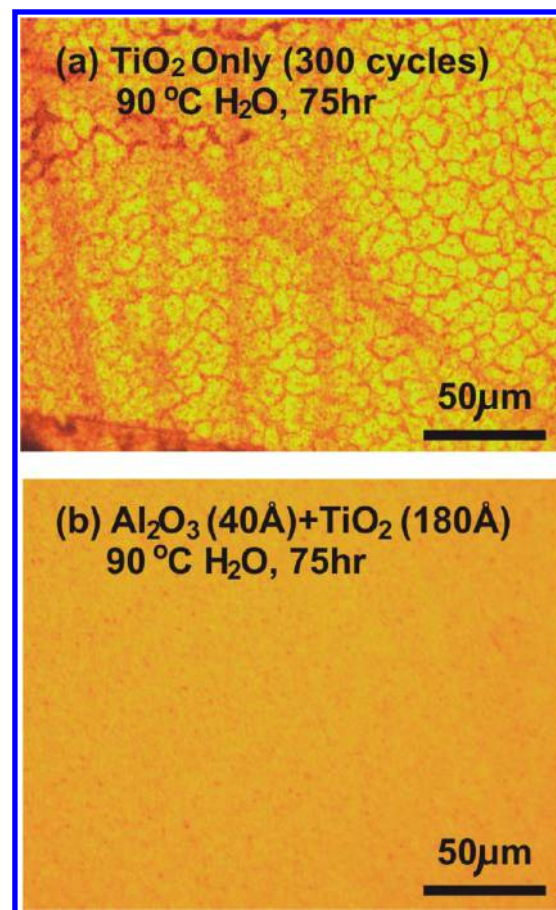

Figure 7. Optical microscope images of copper substrates after 75 h in water at 90 °C with: (a) 300 cycles of TiO_2 ALD at 120 °C; and (b) TiO_2 capping layer with a thickness of 180 Å on Al_2O_3 adhesion layer with a thickness of 40 Å grown at 120 °C.

The defects in the Al_2O_3 films are most likely caused by residual particle contamination. Although the copper substrates were cleaned in a class 100 clean room environment prior to Al_2O_3 ALD, there still may be some particles that adhere to the copper substrate or particles that are not easily removed from the initial copper substrate. The excellent WVTRs measured for Al_2O_3 ALD-coated polymers suggest that the Al_2O_3 films are comparable to glass and do not contain intrinsic defects.[33,34]

C. TiO$_2$ ALD on Copper. Although Al_2O_3 ALD is an excellent barrier film, the Al_2O_3 films are susceptible to water corrosion.[38] In contrast, TiO_2 is much more resilient to water corrosion.[39,40] Consequently, TiO_2 ALD was grown on the copper substrates at 120 °C and then examined using ex situ XPS analysis. The XPS measurements after 300 cycles of $TiCl_4$ and water showed the presence of adventitious carbon C (51.30 at %) together with Cl (1.42 at %), O (30.25 at %), Ti (11.78 at %) and Cu (5.24 at %). On the basis of the previously reported TiO_2 ALD growth rate of 0.6 Å/cycle,[51] the expected TiO_2 film thickness is ~180 Å. The presence of copper in the XPS spectrum indicates either that the TiO_2 film thickness is less than the photoelectron penetration depth of ~50 Å or that the TiO_2 ALD film did not nucleate well on the copper substrates.

AFM results for TiO_2 films on copper substrates also were consistent with nucleation difficulties for TiO_2 ALD. Figure 5a shows a 1 μm × 1 μm AFM scan of a copper substrate after TiO_2 ALD using 300 cycles of $TiCl_4$ and H_2O at 120 °C. The surface is

very rough with a root-mean-square (rms) roughness of 14.0 nm. In comparison, the initial copper substrate had a rms roughness of 5.5 nm. The roughness of the TiO_2-coated substrate is consistent with the nucleation of scattered TiO_2 islands that grow and yield a rough surface.

In contrast to TiO_2 ALD, Al_2O_3 ALD can nucleate readily on the copper substrate. An adhesion layer of Al_2O_3 may facilitate the subsequent TiO_2 ALD. Figure 5b shows an AFM image of a copper surface after depositing a ~40 Å adhesion layer of Al_2O_3 ALD using 40 cycles of TMA and H_2O at 120 °C followed by 300 cycles of $TiCl_4$ and H_2O to grow the TiO_2 coating at 120 °C. This surface has an rms roughness value of 6.0 nm that is nearly identical to the initial copper substrate.

The smoothness of the TiO_2 capping layer demonstrates that the Al_2O_3 adhesion layer can ensure proper nucleation and conformality of the TiO_2 ALD films. Ellipsometery measurements of TiO_2 ALD films grown on the Al_2O_3 adhesion layer on copper were consistent with the previously reported TiO_2 ALD growth rate of 0.6 Å/cycle.[51] In addition, XPS scans performed on the same samples revealed no traces of copper and a Cl/Ti atomic percentage ratio of 0.034. This chlorine concentration is comparable to a previously reported Cl/Ti atomic percentage ratio of 0.047 for TiO_2 ALD using the same conditions.[52]

D. Corrosion Protection of Copper Using Al_2O_3 and TiO_2 ALD. Optical imaging was used to examine the water corrosion of

4597

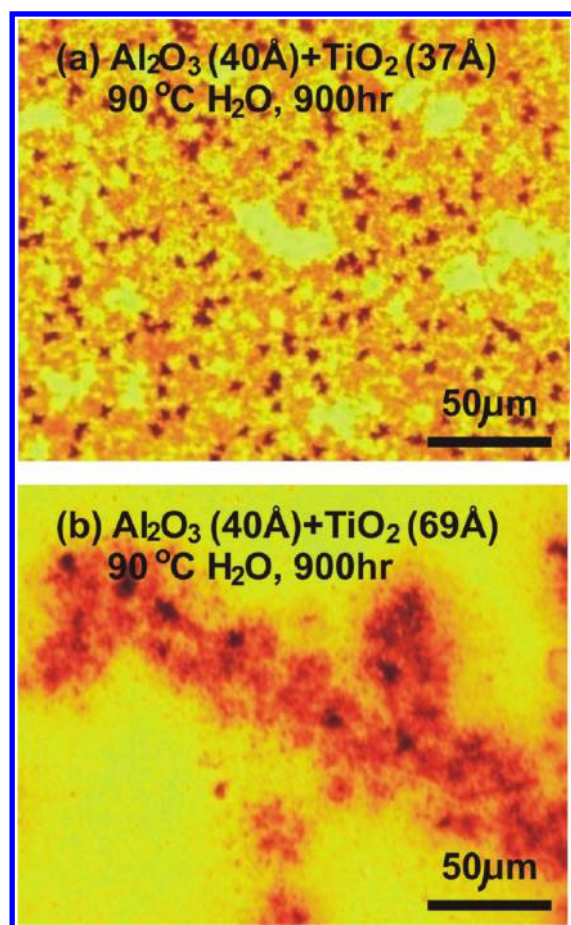dx.doi.org/10.1021/am2009579 |ACS Appl. Mater. Interfaces 2011, 3, 4593–4601

Figure 8. Optical microscope images of copper substrates after 900 h in water at 90 °C with: (a) TiO$_2$ capping layer with a thickness of 37 Å; and (b) TiO$_2$ capping layer with a thickness of 37 Å. The TiO$_2$ capping layers were on Al$_2$O$_3$ adhesion layers with a thickness of 40 Å. TiO$_2$ and Al$_2$O$_3$ ALD were performed at 120 °C.
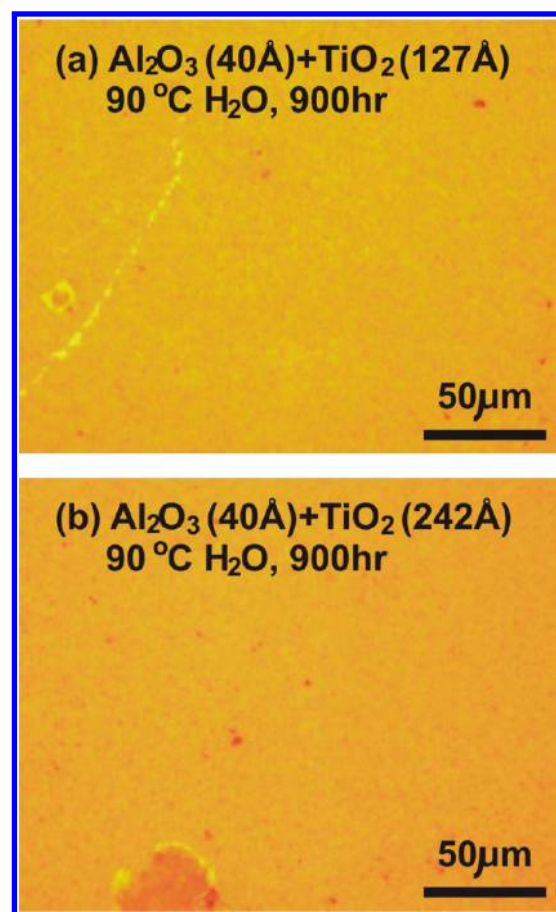

Figure 9. Optical microscope images of copper substrates after 900 h in water at 90 °C with: (a) TiO$_2$ capping layer with a thickness of 127 Å; and (b) TiO$_2$ capping layer with a thickness of 242 Å. The TiO$_2$ capping layers were on Al$_2$O$_3$ adhesion layers with a thickness of 40 Å. TiO$_2$ and Al$_2$O$_3$ ALD were performed at 120 °C.

copper substrates immersed in water at 90 °C. Figure 6a shows the surface of an uncoated copper substrate after immersion in water at 90 °C for 75 h. This copper substrate has corroded significantly leading to discoloring and multiple structured features. In comparison, the original copper substrate was a uniform golden brown color with no structure.

Figure 6b displays the image of a copper substrate coated with 165 cycles of Al$_2$O$_3$ ALD at 120 °C after immersion in water at 90 °C for 75 h. The 165 cycles are sufficient to deposit an Al$_2$O$_3$ thickness of ∼200 Å on the copper substrate. The copper substrate has again corroded and developed many fine features. The Al$_2$O$_3$ film by itself is not capable of protecting the copper substrate from water corrosion.

Figure 7a shows the image of a copper substrate coated with 300 cycles of TiO$_2$ ALD at 120 °C without an Al$_2$O$_3$ adhesion layer after immersion in water at 90 °C for 75 h. This copper substrate is also badly corroded as evidenced by the discoloration and multiple features. The corrosion is expected because the TiO$_2$ film does not nucleate efficiently on the copper substrate. Consequently, there are probably open copper areas on the substrate that begin to corrode very quickly in the hot water.

Water corrosion resistance was observed for TiO$_2$ capping layers on the Al$_2$O$_3$ adhesion layers on copper substrates. Figure 7b displays the image of a copper substrate that was first

coated with an Al$_2$O$_3$ layer thickness of ∼40 Å at 120 °C. Subsequently, TiO$_2$ was grown on the Al$_2$O$_3$ layer using 300 cycles of TiCl$_4$ and H$_2$O at 120 °C to produce a TiO$_2$ layer thickness of ∼180 Å. This sample was much more resistant to corrosion after immersion in water for 75 h at 90 °C.

After establishing that the TiO$_2$ layer was resistant to water corrosion, optical imaging was used to determine the extent of corrosion as a function of TiO$_2$ coating thickness on the Al$_2$O$_3$ layer on copper substrates. TiO$_2$ capping layer thicknesses were explored from 37 Å to 242 Å. The Al$_2$O$_3$ adhesion layers had a thickness of ∼40 Å. All of these samples were immersed in water at room temperature and 90 °C for 900 h.

Optical images of various samples that were immersed in water at 90 °C for 900 h are shown in Figures 8 and 9. The results for the TiO$_2$ thicknesses of 37 and 69 Å in images a and b in Figure 8, respectively, reveal that thinner TiO$_2$ films are insufficient to protect the copper substrate from water corrosion. The copper substrates are discolored and covered with multiple features.

The results for the TiO$_2$ thicknesses of 127 Å and 242 Å in images a and b in Figure 9, respectively, show that the thicker TiO$_2$ films are sufficient to provide a significant degree of protection. Only a few corrosion regions exist. These corroded regions are mostly circular spots that are consistent with corrosion through pinhole defects. The samples in images a and b in
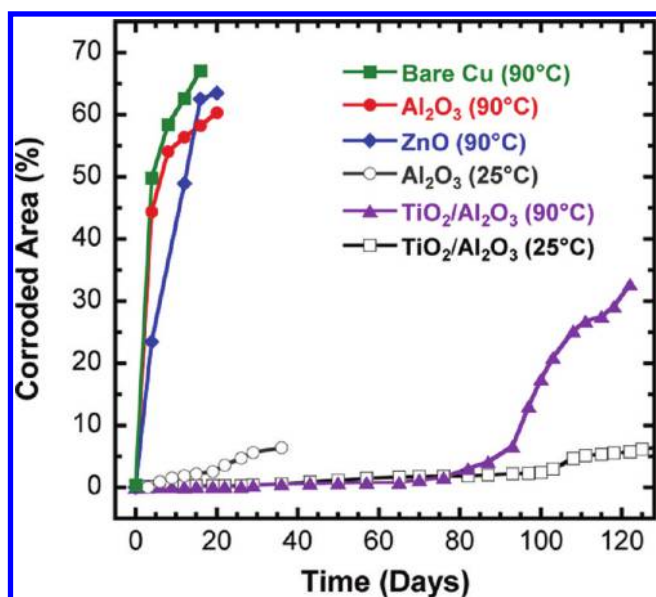
Figure 10. Corroded area on copper substrate derived using ImageJ versus time in water at 25 and 90 °C for bare copper and copper coated with Al_2O_3 ALD, ZnO ALD, and both Al_2O_3 and TiO_2 ALD. The film thicknesses were 200 Å for the Al_2O_3 coating and 250 Å for the ZnO coating. For the TiO_2/Al_2O_3 coating, the Al_2O_3 adhesion layer thickness was 55 Å and the TiO_2 capping layer thickness was 200 Å. All ALD films were grown at 120 °C.

Figure 9 also retain their original golden brown color. These thicker TiO_2 coatings are nearly sufficient to prevent corrosion in water at 90 °C for 900 h.

The corroded area of the copper substrate was quantified using ImageJ processing software during tests lasting over 120 days. The corrosion was quantified by setting a threshold for the darkness of an individual pixel. The golden brown color of the initial copper substrate was set just below the greyscale intensity threshold. The dark, discolored corroded regions of the substrate were then all darker than the greyscale intensity threshold. After setting this threshold, the corroded area of the copper substrates could be monitored versus time.

Figure 10 shows the results from this ImageJ processing for a variety of coated copper substrates including Al_2O_3, TiO_2, TiO_2/Al_2O_3 and ZnO. These samples were immersed in hot water at 90 °C. Some comparative results are also shown for tests performed in water at room temperature. Figure 10 reveals that the copper substrates coated with an Al_2O_3 adhesion layer with a thickness of ∼55 Å and a TiO_2 capping layer with a thickness of ∼200 Å can survive for ∼80 days prior to any observed corrosion in water at 90 °C. This same coating can survive for >100 days in water at 25 °C with a much slower corrosion rate after reaching the threshold for some observable corrosion. The Al_2O_3 adhesion layer with a thickness of 55 Å was grown using 50 cycles of TMA and water. This slightly larger adhesion layer thickness should not affect the TiO_2 ALD nucleation or the corrosion rate.

In contrast, Figure 10 reveals that the copper substrates covered with only an Al_2O_3 film with a thickness of ∼200 Å or a ZnO film with a thickness of ∼250 Å corrode almost immediately in hot water at 90 °C. For both of these coatings, the corroded areas are >50% after 5 days. These results are only marginally better than the uncoated copper substrate in water at 90 °C. The copper substrate with an Al_2O_3 film with a thickness
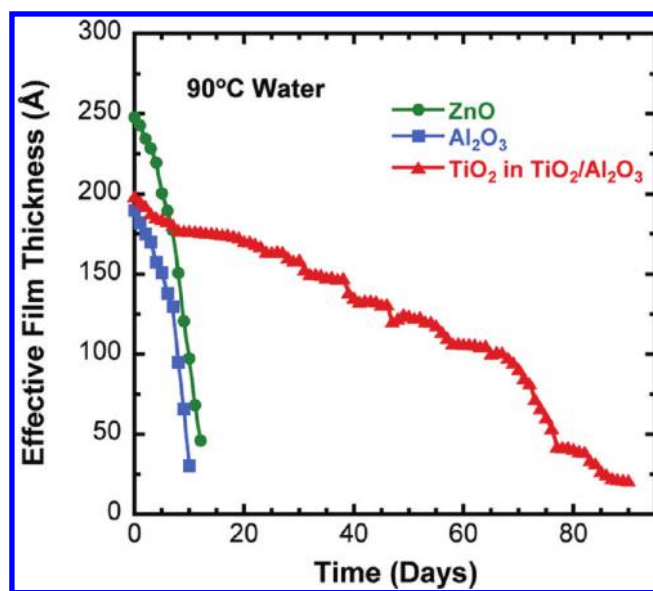

Figure 11. Effective film thickness on copper substrate versus time in 90 °C water for Al_2O_3, ZnO, and TiO_2/Al_2O_3 ALD coatings. For the TiO_2/Al_2O_3 coating, the Al_2O_3 adhesion layer thickness was 55 Å and the TiO_2 capping layer thickness was 200 Å. All ALD films were grown at 120 °C.

of ∼200 Å in water at room temperature corrodes much more slowly. Corrosion is observed from nearly the beginning. However, the corrosion rate is much slower than the corrosion rate at 90 °C.

The optical images also revealed that scratched regions of the uncoated or coated copper substrate led to more darkening and corrosion than unscratched regions of the substrate. The scratched regions displayed more corrosion both before and after coating. The scratches probably introduce more active surface sites that are more susceptible to chemical change.

E. Dissolution of Al_2O_3, ZnO and TiO_2/Al_2O_3 ALD Films. The best corrosion resistance in water at 90 °C was obtained with copper substrates covered with an Al_2O_3 adhesion layer with a thickness of 55 Å and then coated with a TiO_2 capping layer with a thickness of ≥200 Å at 120 °C. However, these coated copper substrates displayed corrosion after >80 days. This corrosion may be related to the dissolution of the TiO_2/Al_2O_3 films. To test this idea, ellipsometry was used to measure the thickness of the TiO_2/Al_2O_3 film versus time during immersion in water at 90 °C.

Figure 11 displays the "effective" film thickness measured by ellipsometry versus time for Al_2O_3, ZnO and TiO_2/Al_2O_3 films during immersion in water at 90 °C. The film thickness is "effective" because the corrosion does not produce perfectly homogeneous films. There are some corrosion pits as evidenced by the optical microscope images in Figures 8 and 9. In addition, the effective film thickness is shown for only the TiO_2 component of the TiO_2/Al_2O_3 film. The separation of the TiO_2 and Al_2O_3 layers was accomplished by assuming an Al_2O_3 adhesion layer thickness of 55 Å under the TiO_2 capping layer in the fit of the ellipsometry data.

Figure 11 shows that the Al_2O_3 and ZnO films dissolve very quickly in less than 10−15 days. In contrast, the TiO_2 capping layer on the Al_2O_3 adhesion layer starts with a thickness of ∼200 Å and progressively dissolves over ∼90 days. The loss of the TiO_2 layer thickness is fairly linear and suggests that the TiO_2 layer is
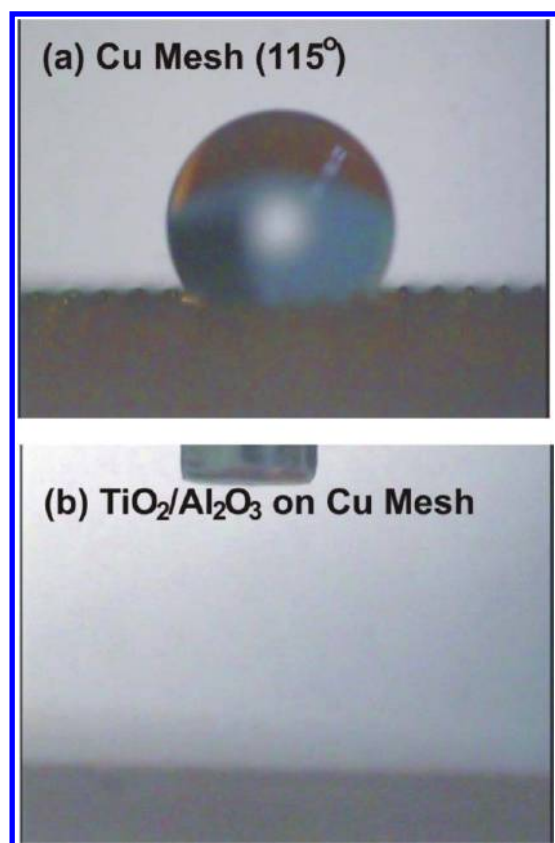
Figure 12. Water contact angle measurements for: (a) bare woven copper mesh with 5 μm wire size; and (b) copper mesh with TiO_2 capping layer thickness of 100 Å on Al_2O_3 adhesion layer thickness of 55 Å. The TiO_2 and Al_2O_3 ALD films were grown at 120 °C.

dissolving in water at 90 °C with zero-order kinetics. Additional experiments with different thicknesses of the TiO_2 capping layer on the Al_2O_3 adhesion layer could confirm the zero-order dissolution kinetics.

There are correlations between the corroded area percentage results in Figure 10 and the effective film thicknesses in Figure 11. For the TiO_2/Al_2O_3 film, the corroded area starts to increase when the TiO_2 layer is removed by dissolution. This correlation indicates that the corrosion resistance is determined by the TiO_2 ALD film thickness. The TiO_2/Al_2O_3 coating can protect the copper substrate until the TiO_2 capping layer on the Al_2O_3 adhesion layer is dissolved after ~90 days in water at 90 °C.

F. Wetting Properties of TiO$_2$ ALD-Coated Copper. H_2O wetting of the TiO_2 capping layers on the Al_2O_3 adhesion layers on copper were investigated using the sessile drop method to determine the water contact angle. The TiO_2 capping layers on the Al_2O_3 adhesion layers were deposited at 120 °C on copper meshes with 50 μm wire diameters. The size of the water droplet for the contact angle measurements was limited to 1 μL to avoid gravitational effects. All TiO_2 samples were protected from ultraviolet (UV) light exposure prior to testing. This precaution was necessary since the wetting properties of TiO_2 are sensitive to UV light.[53]

Images a and b in Figure 12 show the results after adding a water droplet to the copper wire meshes before and after the deposition of TiO_2 capping layers on the Al_2O_3 adhesion layers. Figure 12a shows that a large contact angle of 115° is measured

on the uncoated copper wire mesh. This large contact angle is typical for substrates where the water bridges the tops of the substrate features. The water droplet rests on flat solid tops and air gaps between them as described by the Cassie—Baxter model.[54] According to this model, the apparent contact angle is determined by contributions from both the solid tops and the air gaps.

Figure 12b shows the result after adding a water droplet to the surface of the TiO_2-coated copper wire mesh. The TiO_2-coated copper mesh rapidly and completely wicks the water droplet. This wettability is consistent with a low contact angle and the presence of strong capillary forces. A slight difference in wetting speed was observed when water droplets were placed on dry versus wet copper meshes. Slower water spreading was observed on wet meshes. These TiO_2-coated copper wire meshes should be very useful for heat exchangers employing thermal transport based on water adsorption and desorption.

4. CONCLUSIONS

Al_2O_3 and TiO_2 ALD were used to fabricate ultrathin protective coatings on copper to prevent water corrosion. Al_2O_3 or TiO_2 ALD alone was not effective to prevent water corrosion of copper. Although the Al_2O_3 ALD films covered copper uniformly with a nearly pinhole-free film, the Al_2O_3 films easily dissolved in water at 90 °C. The TiO_2 ALD films had nucleation difficulties and did not completely cover the underlying copper substrate leading to facile copper corrosion. In contrast, a composite coating formed by an Al_2O_3 adhesion layer on copper and then a TiO_2 capping layer on the Al_2O_3 adhesion layer proved to be very resistant to water corrosion.

Optical microscopy images revealed that TiO_2 capping layers as thin as ~200 Å on Al_2O_3 adhesion layers with a thickness of ~55 Å could prevent copper corrosion from water exposures at 90 °C for ~80 days. Ellipsometry measurements revealed that Al_2O_3 films with a thickness of ~200 Å dissolved in water at 90 °C in ~10 days. In comparison, TiO_2 capping layers with thicknesses of ~200 Å on Al_2O_3 adhesion layers with thicknesses of ~55 Å protected the underlying copper substrate for ~90 days in water at 90 °C. The TiO_2 ALD coatings were also hydrophilic and facilitated H_2O wetting of copper wire mesh substrates.

■ AUTHOR INFORMATION

Corresponding Author
*E-mail: steven.george@colorado.edu.

■ REFERENCES

(1) Leidheiser Jr., H. *The Corrosion of Copper, Tin, and Their Alloys*; John Wiley and Sons: New York, 1971.

(2) Feng, Y.; Teo, W. K.; Siow, K. S.; Hsieh, A. K. *Corros. Sci.* **1996**, *38*, 387.

(3) Feng, Y.; Teo, W. K.; Siow, K. S.; Tan, K. L.; Hsieh, A. K. *Corros. Sci.* **1996**, *38*, 369.

(4) Jeon, B.; Sankaranarayanan, S.; van Duin, A. C. T.; Ramanathan, S. *J. Chem. Phys.* **2011**, *134*.

(5) Pehkonen, S. O.; Palit, A.; Zhang, X. *Corrosion* **2002**, *58*, 156.

(6) Sobue, K.; Sugahara, A.; Nakata, T.; Imai, H.; Magaino, S. *Surf. Coat. Technol.* **2003**, *169*, 662.

(7) Feng, Y.; Siow, K. S.; Teo, W. K.; Tan, K. L.; Hsieh, A. K. *Corrosion* **1997**, *53*, 389.

(8) Boulay, N.; Edwards, M. *Water Res.* **2001**, *35*, 683.

(9) Lau, K. H.; Sanjurjo, A.; Wood, B. J. *Surf. Coat. Technol.* **1992**, *54*, 234.

(10) Sanjurjo, A.; Wood, B. J.; Lau, K. H.; Tong, G. T.; Choi, D. K.; McKubre, M. C. H.; Song, H. K.; Church, N. *Surf. Coat. Technol.* **1991**, *49*, 110.

(11) Itoh, M.; Nishihara, H.; Aramaki, K. *J. Electrochem. Soc.* **1994**, *141*, 2018.

(12) Itoh, M.; Nishihara, H.; Aramaki, K. *J. Electrochem. Soc.* **1995**, *142*, 3696.

(13) Yamamoto, Y.; Nishihara, H.; Aramaki, K. *J. Electrochem. Soc.* **1993**, *140*, 436.

(14) Brusic, V.; Frisch, M. A.; Eldridge, B. N.; Novak, F. P.; Kaufman, F. B.; Rush, B. M.; Frankel, G. S. *J. Electrochem. Soc.* **1991**, *138*, 2253.

(15) Wu, Y. C.; Zhang, P.; Pickering, H. W.; Allara, D. L. *J. Electrochem. Soc.* **1993**, *140*, 2791.

(16) Youda, R.; Nishihara, H.; Aramaki, K. *Corros. Sci.* **1988**, *28*, 87.

(17) Brusic, V.; Angelopoulos, M.; Graham, T. *J. Electrochem. Soc.* **1997**, *144*, 436.

(18) Cicileo, G. P.; Rosales, B. M.; Varela, F. E.; Vilche, J. R. *Corros. Sci.* **1999**, *41*, 1359.

(19) Tallman, D. E.; Spinks, G.; Dominis, A.; Wallace, G. G. *J. Solid State Electrochem.* **2002**, *6*, 73.

(20) Lin, Y.; Yasuda, H. *J. Appl. Polym. Sci.* **1996**, *60*, 543.

(21) Patil, S.; Sainkar, S. R.; Patil, P. P. *Appl. Surf. Sci.* **2004**, *225*, 204.

(22) George, S. M. *Chem. Rev.* **2010**, *110*, 111.

(23) Elam, J. W.; Routkevitch, D.; Mardilovich, P. P.; George, S. M. *Chem. Mater.* **2003**, *15*, 3507.

(24) Dillon, A. C.; Ott, A. W.; Way, J. D.; George, S. M. *Surf. Sci.* **1995**, *322*, 230.

(25) Ott, A. W.; Klaus, J. W.; Johnson, J. M.; George, S. M. *Thin Solid Films* **1997**, *292*, 135.

(26) Puurunen, R. L. *J. Appl. Phys.* **2005**, *97*, 121301.

(27) Marin, E.; Lanzutti, A.; Guzman, L.; Fedrizzi, L. *J. Coat. Technol. Res.* **2011**, *8*, 655.

(28) Matero, R.; Ritala, M.; Leskela, M.; Salo, T.; Aromaa, J.; Forsen, O. *J. Phys. IV* **1999**, *9*, 493.

(29) Ritala, M.; Leskela, M.; Nykanen, E.; Soininen, P.; Niinisto, L. *Thin Solid Films* **1993**, *225*, 288.

(30) Shan, C. X.; Hou, X. H.; Choy, K. L. *Surf. Coat. Technol.* **2008**, *202*, 2399.

(31) Shan, C. X.; Hou, X.; Choy, K. L.; Choquet, P. *Surf. Coat. Technol.* **2008**, *202*, 2147.

(32) Groner, M. D.; Elam, J. W.; Fabreguette, F. H.; George, S. M. *Thin Solid Films* **2002**, *413*, 186.

(33) Carcia, P. F.; McLean, R. S.; Groner, M. D.; Dameron, A. A.; George, S. M. *J. Appl. Phys.* **2009**, *106*, 023533.

(34) Carcia, P. F.; McLean, R. S.; Reilly, M. H.; Groner, M. D.; George, S. M. *Appl. Phys. Lett.* **2006**, *89*, 031915.

(35) Groner, M. D.; George, S. M.; McLean, R. S.; Carcia, P. F. *Appl. Phys. Lett.* **2006**, *88*, 051907.

(36) Cooper, R.; Upadhyaya, H. P.; Minton, T. K.; Berman, M. R.; Du, X. H.; George, S. M. *Thin Solid Films* **2008**, *516*, 4036.

(37) Minton, T. K.; Wu, B. H.; Zhang, J. M.; Lindholm, N. F.; Abdulagatov, A. I.; O'Patchen, J.; George, S. M.; Groner, M. D. *ACS Appl. Mater. Interfaces* **2010**, *2*, 2515.

(38) Dameron, A. A.; Davidson, S. D.; Burton, B. B.; Carcia, P. F.; McLean, R. S.; George, S. M. *J. Phys. Chem. C* **2008**, *112*, 4573.

(39) Sun, Q. F.; Yu, H. P.; Liu, Y. X.; Li, J. A.; Lu, Y.; Hunt, J. F. *Holzforschung* **2010**, *64*, 757.

(40) Taruta, S.; Watanabe, K.; Kitajima, K.; Takusagawa, N. *J. Non-Cryst. Solids* **2003**, *321*, 96.

(41) Elam, J. W.; Groner, M. D.; George, S. M. *Rev. Sci. Instrum.* **2002**, *73*, 2981.

(42) Liu, C. *Adv. Mater.* **2007**, *19*, 3783.

(43) Ritala, M.; Leskela, M.; Niinisto, L.; Haussalo, P. *Chem. Mater.* **1993**, *5*, 1174.

(44) Elam, J. W.; Schuisky, M.; Ferguson, J. D.; George, S. M. *Thin Solid Films* **2003**, *436*, 145.

(45) Cocke, D. L.; Schennach, R.; Hossain, M. A.; Mencer, D. E.; McWhinney, H.; Parga, J. R.; Kesmez, M.; Gomes, J. A. G.; Mollah, M. Y. A. *Vacuum* **2005**, *79*, 71.

(46) Zhang, Y. D.; Bertrand, J. A.; Yang, R. G.; George, S. M.; Lee, Y. C. *Thin Solid Films* **2009**, *517*, 3269.

(47) ImageJ. http://rsbweb.nih.gov/ij/.

(48) Groner, M. D.; Fabreguette, F. H.; Elam, J. W.; George, S. M. *Chem. Mater.* **2004**, *16*, 639.

(49) Wind, R. A.; George, S. M. *J. Chem. Phys. A* **2010**, *114*, 1281.

(50) Wilson, C. A.; Grubbs, R. K.; George, S. M. *Chem. Mater.* **2005**, *17*, 5625.

(51) Aarik, J.; Aidla, A.; Mandar, H.; Sammelselg, V. *J. Cryst. Growth* **2000**, *220*, 531.

(52) Triani, G.; Campbell, J. A.; Evans, P. J.; Davis, J.; Latella, B. A.; Burford, R. P. *Thin Solid Films* **2010**, *518*, 3182.

(53) Ye, Q.; Liu, P. Y.; Tang, Z. F.; Zhai, L. *Vacuum* **2007**, *81*, 627.

(54) Roach, P.; Shirtcliffe, N. J.; Newton, M. I. *Soft Matter* **2008**, *4*, 224.